NISS

Link Travel Time Estimation with Imputed Signal Control Information

Piyushimita Thakuriah

Technical Report Number 52
October, 1996

National Institute of Statistical Sciences
19 T. W. Alexander Drive
PO Box 14006
Research Triangle Park, NC 27709-4006
www.niss.org

Link Travel Time Estimation with Imputed Signal Control Information [1]

Piyushimita (Vonu) Thakuriah
Research Fellow
National Institute of Statistical Sciences
PO Box 14162, Research Triangle Park, NC 27709-4162

[1]This work was supported by the National Science Foundation's Division of Mathematical Sciences Grant Numbers 9313013 and 9208758. The author would also like to thank the ADVANCE project for making the data available and to acknowledge the encouragement of Ashish Sen and Alan Karr and the help of Xia-Quon Zhu.

1 INTRODUCTION

One of the major functions of an Advanced Traveler Information System (ATIS) is route guidance. A key sub-problem of route guidance is the estimation of travel times on links in a network. The link travel time estimation problem is to estimate the travel time that would be incurred by a vehicle entering the link at some time t. Thus far, there have been two approaches to the link travel time estimation problem: (i) dynamic traffic assignment and (ii) statistical approaches based on real or simulated travel time data. In this paper, we present some investigations of the link travel time estimation probe via the second approach. Direct measurements of travel times has recently become possible with the advent of network surveillance technologies such as probe vehicles and video cameras that are capable of matching a vehicle at two different locations.

Link travel times have been estimated as a univariate time series (Liu and Sen, 1996) or by regression relationships from travel time and other related data (Rouphail and Dutt, 1995). In this paper, we take the view that link travel times have a number of important covariates and that it is important to include information on these covariates directly in the estimation process. Under recurrent congestion on signalized arterials, two fundamental covariates of link travel times are the interactive effects of signalization (vehicle arrivals in relation to signal control phases) and volume levels. With this approach, we now devote our attention to the effects of these covariates on link travel time estimates and ways in which one can include them in travel time estimation process.

However, for an ATIS or an Advanced Traffic Management System (ATMS) to make direct observations on all important covariates on an area-wide basis would imply prohibitive costs on system design, hardware and software. Area-wide data on volumes and the signal phases on a continuous clock are not likely to be readily available, at least in the near future.

Therefore, the purpose of this paper is to examine if we can infer information on important covariates on which we do not have measurements, from travel time data on which we *do* have measurements. We consider the case of inferring from travel time data, the status of signal control alone, leaving the problem of inferring volume levels from travel times as a subject for future research. We then use the estimated sequence of signal cycles for the purpose of link travel time estimation and also for the dynamic 'real-time' prediction of future link travel times.

There are three major effects on the estimates of travel time if the effects of signalization is ignored (Thakuriah, *et al.*, 1996) in the estimation of expected link travel time. First, the estimate would be of high variance and second, the resultant estimate may be biased. The third, and perhaps the main reason is to be considered in the context of travel time estimation on routes r that include link ℓ which is a requirement in the route guidance function of an ATIS. Under recurrent congestion, one may conjecture that errors in estimating expected link travel times would cancel out over a route. In fact, if travel times on links over a route were independent, one would expect this to occur by the Law of Large Numbers. However, volume and progression effects cause travel time estimates on links along a route to be dependent, implying that errors in estimating link travel times may persist over a route. The lack of independence requires us to 'correct' the estimate of the expected link travel time for factors that causes this dependence. The inclusion of the effect of signalization in a model of link travel time estimation would serve this corrective purpose.

Therefore, in this paper, we make imputations about the cyclical sequence of signal control in terms of clock time, directly from observations of link travel times, tt, and clock time, t, of vehicle exit from a link. We do so, we first estimate average cycle lengths and then use these estimates along with link travel time and vehicle exit time data to estimate the sequence of signal cycles on a continuous clock. Then given these imputed values of signal control, we estimate the expected travel time at time t and also predict the travel time for a vehicle entering a link at a future time $t + \delta$.

While the signal cycle imputation algorithm has been presented in the context of off-line and dynamic link travel time prediction, it could be used for other purposes. For example, the method could be used by an ATMS to monitor signal malfunction in real-time. It could also be used for the purpose of long-term signal control parameter resetting in order to optimize traffic flow. Finally, it could be used to generate 'data' to input into various dynamic traffic simulations that model the effects of ATIS and ATMS.

The paper is organized as follows: in Section 2, we present some relevant background information and define the problem of estimating signal control attributes from realizations of travel time. We also describe the data used for the empirical investigations. In Section 3, we define our approach to estimating average cycle lengths and the algorithm for estimating the sequence of signal cycle lengths on a continuous clock. We present the applications and related discussion in Section 4. We then make some concluding remarks.

2 LINK TRAVEL TIME ESTIMATION

In this section, we explore the relationships between travel time and the two fundamental covariates of volume and signalization. There are three time trends in travel time observations on signalized arterials: a day-of-week, time-of-day and a periodic pattern imposed by signalization (Sen and Thakuriah, 1995). Under recurrent congestion, we could think about these three trends as a hierarchy of conditioning information for travel time estimation. In this section, we present an empirical example of travel time estimation when we condition on knowledge of day-type, time-of-day and signalization. Let tt_i be the travel time of the ith vehicle that exited link ℓ at time t (measured on a continuous clock). We are interested in the relationship between tt_i and ρ_i ($\rho_i = t_i \text{modulo}(r_i)$ is termed as relativized exit time where r_i is the start of the cycle (as well as of the red phase) in which the ith vehicle exited). The purpose of the example is to empirically illustrate the nature of the relationship between tt and ρ and to examine the effect of including signal information on variability in travel time estimates. In Section 2.1, we discuss the way in which knowledge of the relationship between tt and ρ allows imputation of the sequence of signal cycles.

The data used for all empirical investigations presented in this paper were collected by field tests as part of the evaluation of ADVANCE, an ATIS demonstration project (Boyce *et al*, 1994), during the summer of 1995 in the northwest suburbs of Chicago. The link travel time data were transmitted in real-time from specially-equipped probe vehicles that were driven by paid drivers. Data were collected on links along several routes. While the probe vehicles collected data on several variables, we have used only link travel times and link exit times in this study. The entry and exit points of the three study links were also monitored by video surveillance cameras for 10

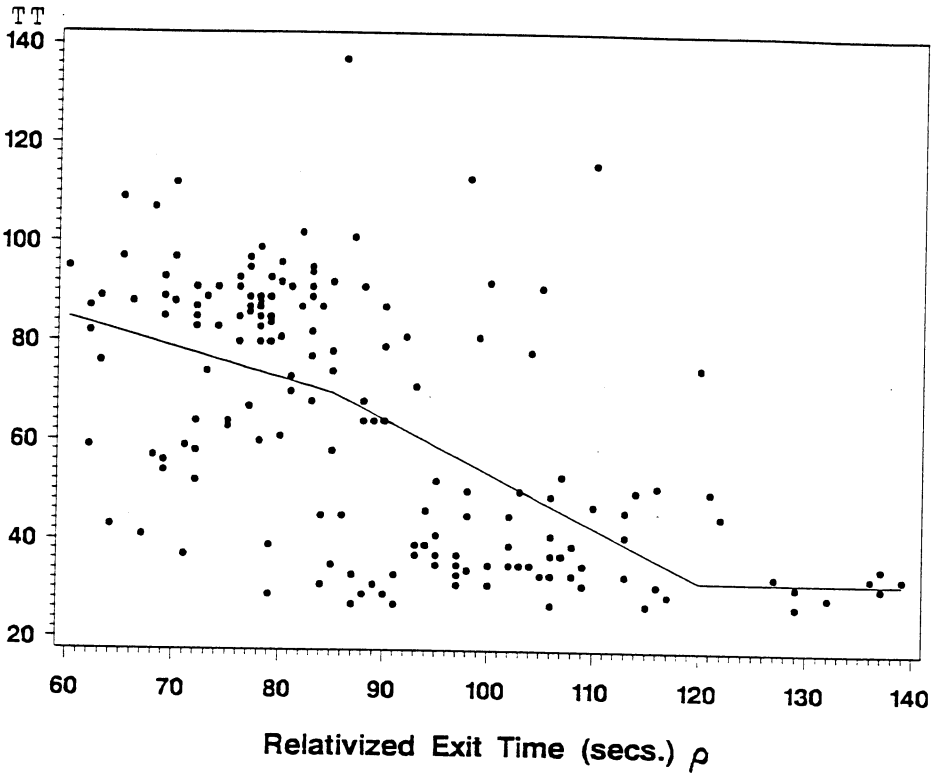

Figure 1: Piece-wise linear fit of tt and ρ on a link conditioned on day-type and time-of-day.

days, that filmed the signal control at the both downstream and upstream intersections of the three study links (data on the sequence of signal cycles and phases were not available from any other source). Almost all links in the routes covered by probes, including the three study links, are part of a Closed Loop Signal Control system.

For the empirical analysis presented in this section, we have used actual data on signals to compute ρ. However, the signal data will be used in other empirical analysis in this paper only for comparative purposes and not as input into any actual computations.

Figure 1 shows a fit and Table 1 gives the estimates from the model

$$tt_i = \alpha + \beta_1 \rho_i + \beta_2[\max(\rho_i - \mu_1), 0] + \beta_3[\max(\rho_i - \mu_2), 0] + \epsilon_i \quad (1)$$

s.t.

$$\beta_1 + \beta_2 + \beta_3 = 0.$$

Estimates:	$\hat{\alpha}$=123.71	$\hat{\beta}_1 = -0.60$	$\hat{\beta}_2 = -0.47$	$\hat{\beta}_3 = 1.08$
Break Pts.	$\hat{\mu}_1 = 85$ secs.	$\hat{\mu}_2 = 120$ secs.		
Slopes:	Part 1: -0.60	Part 2: -1.08	Part 3: 0	
$\hat{tt}(\bar{g})$	87.71 secs.			
Fit:	s=16.23	R^2=.74		

Table 1: Estimates from model of travel time as a function of relativized time. $\hat{tt}(\bar{g})$ is the predicted travel time at the average start time of the green phase, $\bar{g}$.

The model was estimated by nonlinear least squares and the two break points, μ_1 and μ_2, that gives the transition from one regime to the next were parameters in the model. The break points are estimated to be $\hat{\mu}_1 = 85$ seconds (after the start of the cycle) and $\mu_2 = 120$ seconds. The estimated travel time, at $\rho = 60$ seconds (or the average length of the red phase) is about 88 seconds. The estimated free-flow travel time obtained by dividing link length by the speed limit is of the order of 28 seconds. Hence, the estimated travel time at $\rho = 60$ is (free flow time) + $\bar{R}$, where $\bar{R}$ is the average length of the red phase.

The pattern of points in Figure 1 is messy. However, the points at the lower left corner and the upper right corner are not outliers for the following reasons:

1. If there is no queue at the start of the green phase and vehicles arrive at the time the phase changes from red to green, then one can expect vehicles departing shortly after the end of the red phase to incur travel times that are about the same as free-flow travel times.

2. Although the observations in the upper right corner occur late in the cycle, they are still relatively high because of oversaturation conditions.

3. The Closed Loop Signal System (CLSS) adds to the noisiness in the 'unusual observations' when we group data over all cycles as in Figure 1 in the following ways: (i) the lower left-hand points may actually be toward the end of a short cycle; in that case, the low travel time values are quite reasonable (ii) the upper right-hand points may be exit times during the middle or even the start of some long cycle, although these points are toward the end of the 'average' cycle.

Therefore, the interactive effects of signalization and volumes lead vehicles that depart right after the onset of the green phase to encounter higher travel times than those exiting at other periods of time.This analysis leads us to believe that travel time is a non-increasing function, $f(\rho)$, of ρ, with a flat tail because there is clearly a lower bound to this function, imposed by the minimu realistic time at which the distance can be traversed. We discuss the nature of this function and its importance in the signal imputation problem in Section 2.1.

2.1 FUNCTION $f(\rho)$

In this section, we introduce the signal cycle imputation problem in detail. Let $\{tt_1, tt_2, \ldots, tt_n\}$ be a vector of travel times on link ℓ generated on day d, and $\{t_1, t_2, \ldots, t_n\}$ be the corresponding vector of link exit times. Also let $\{v_1, v_2, \ldots, v_n\}$ be the vector of vehicle velocity at the time of link exit.

We state two conditions:

Condition 1: All vehicles travel at constant speed except when they are part of a queue.

Condition 2: The time headway between two vehicles is a decreasing function of the velocity of the second vehicle.

Revised Condition 2: Assume two groups of vehicles, a and b, with two vehicles (1 and 2) in each group. Then

$$v_1^{(a)} > v_1^{(b)} \Rightarrow t_2^{(a)} - t_1^{(a)} \geq t_2^{(b)} - t_1^{(b)}. \tag{2}$$

Lemma. Under Conditions 1 and 2, tt is a non-increasing function of ρ.

Considering tt as a function of relativized exit time ρ allows us to get a handle on the signal cycle imputation problem. This is because of the following: *if we can realistically estimate the ρ that $tt(t)$ corresponds to, then we can map the exit time t of the vehicle recorded on a continuous clock to the time elapsed after the start of the cycle in which the vehicle exited. That cycle start time is then assigned the continuous clock time $t - \rho$.*

However, this mapping process is affected by the second fundamental covariate of link travel time, volume. The function that relates tt to ρ is dependent on volume. Volume acts on the relationship by scaling the function by a scale factor, Δ. This scaling leads to a family of functions f. Knowledge of volume at time t allows us to determine which of this family of functions is pertinent for the mapping of a particular tt to ρ.

We illustrate the nature of the scale function Δ, by considering a deterministic model of vehicular link travel time. The measure of volume considered here is $O_v = A_v - D_v$, where A_v is cumulative arrivals upto the arrival time of vehicle v and D_v denotes cumulative departures. As in Section 2, we decompose tt_v into

$$tt_v = cr_v + d_v \tag{3}$$

where cr_v is the cruise time of vehicle v and d_v is intersection delay. Following are the assumptions of the deterministic model:

1. the signalized approach is a queuing system
2. the queuing system can discharge a fixed number of vehicles in one cycle; cycle capacity is fixed and signal cycle length and green splits are fixed from cycle to cycle
3. service time per vehicle is constant
4. FIFO queuing discipline
5. downstream links have infinite storage.

The delay term, d_v, can be decomposed as

$$d_v = \delta([g_v - t_v] + a) + (O_v \times s) + \left[\text{int}\left(\frac{O_v}{\text{cap}}\right) \times R\right] \tag{4}$$

where O_v is the queue in front of v, s is the service time per vehicle (in seconds), cap is cycle capacity (vehicles/cycle), R is the length of red phase (seconds), a is a constant of acceleration (feet/second), g_v is start of green phase of cycle in which v arrived, t_v is the arrival time of v (in continuous clock) and

$$\delta = \begin{cases} 1 & \text{if} \quad r_v \leq t_v < g_v, \\ 0 & \text{if} \quad g_v \leq t_v < c_v \end{cases}$$

where r_v is the start of the red phase (also the cycle) in which the vehicle arrived and c_v marks the end of the cycle. Therefore, d_v has two components:

1. N red times of length R, during which no vehicle in the queue is serviced and where N is the number of full green times G needed to service O_v vehicles from the intersection;
2. since service time (s) for each vehicle is constant, the vehicle has to wait ($O_v \times s$) of green times to clear O_v vehicles through the available green times.

Also, assuming constant free flow speed and vehicle lengths, cr_v decreases linearly with O_v.

Let $f_r(\rho)$ be the function that relates tt to ρ in undersaturated cycles (when the arrival volumes are less than cycle discharge capacity) and when the arrivals are uniformly distributed in the red and green phases. The delay incurred under these conditions are uniform or red phase delay. If tt_v and O_v are known and O_v is positive, then we can find out the appropriate scale factors. In the deterministic model given in expressions (3), ρ_v corresponding to tt_v is completely determined if tt_v and O_v are known and if $O_v > 0$. In that case, the second term in (4) gives $\rho_v = (O_v \times s)\text{modulo}(G)$. This is irrespective of multiple cycle failures that may be incurred by v (that is, when O_v is much larger than capacity). Therefore, the quantity $(O_v \times s)\text{modulo}(G)$ gives the horizontal scale Δ^h. On the other hand, if $O_v = 0$, then knowledge of tt_v and O_v is completely uninformative about ρ_v. We suggest a way to obviate the difficulty posed by $O_v = 0$ in Section 3.2. The entire expression (3) gives the vertical shift, Δ^v from $f_r(\rho)$ to $f'(\rho)$, the function pertinent for O_v.

Once the relevant function $f(\rho)$ pertaining to the set of observations tt and t are known, we can assign a ρ value to tt by straightforward inverse transformation or some other method. We describe the method used for this purpose in Section 3.2. Then once we know ρ_i for tt_i and t_i, we know r_i or the clock time of the start of the cycle when the ith vehicle exited the link.

However, in an application of this approach to our data, we have two problems. First, we have no volume information at time t and second, the link travel time data that we have used for empirical analysis were collected in an area with a Closed Loop Signal Control System, as noted already in Section 2. In a demand-actuated signal control system, the problem of imputing signal cycles become more difficult because all three attributes — signalization, volume and travel times — affect each other. The cycle start times on the study link are aperiodic. By controlling the cycle capacity of upstream links, the signal control system affects volume on a link. Volume on a link, in turn, affects available discharge capacity by extending green phases and cycle lengths, both of which affects travel times. If delay times are high and cycle failure occurs, the volume on a link in future cycles are affected. Travel times are also affected by signal progression. Therefore, if only travel times are known, then there are two unknowns — volume and the status of the signal control system on a continuous clock operational during the clock time t at which the travel time measurement was made. But because all three attributes are related to one another, knowledge of two should allow inference of the third.

Since we do not have information on volume, in this paper, we take a 'minimalist' approach and attempt to find out if the sequence of signal control events (start times of cycles and phases) can be inferred from travel time data alone, by controlling for the second fundamental covariate of travel time, that is, volume. That is, we try to approximate all volume situations with the same

simulated function $f_r(\rho)$ that is relevant functions for uniform or red phase delay. The simulated function is discussed in Section 3.2 and is an attempt to replicate the function presented in Figure 1, where we used the actual signal data. Volume is 'controlled' on the link on which we apply the methods considered in this paper in two ways: (i) the upstream links 'holds back' traffic so that traffic arriving on the study link from upstream links is almost always cleared by the available discharge capacity of the study link (ii) the cross-street at the downstream end of the study link is not highly congested so that green phases and cycle lengths on the study link can be extended, thus avoiding cycle failure on the study link (iii) the average signal cycle length changes at 4 p.m. to accommodate arriving demand in the direction of heavy traffic; therefore, in the signal cycle imputation applications and resultant travel time estimation and predictions, we have considered data reported by probe vehicles after 4 p.m. and (iv) our applications are for the peak period only.

3 ESTIMATION OF SIGNAL CONTROL ATTRIBUTES

In this section, we discuss the estimation of travel time and prediction of travel times at some future time by imputing information on the time-varying sequence of signal cycles. One of the inputs into the algorithm for signal cycle sequence tracking is the average cycle length. We obtain the average cycle length from tt alone in Section 3.1. We then present the details of the cycle imputation algorithm based on tt in Section 3.2.

3.1 INFERRING CYCLE LENGTH FROM TRAVEL TIME DATA

Because the probe-generated travel times data are unequally spaced and extremely sparse, most well-established spectral methods are not useful in inferring the periodicity due to signal control from probe travel time data alone. In this section, we present a way of inferring the average signal cycle length on a signalized arterial based on probe data alone.

As indicated earlier, under recurrent congestion, there are three major time patterns in link travel times. There are the day-of-week, time-of-day and the short-lived periodicity induced by signalization. If we could subtract out the day and time of day effects from a model of travel times, then the residual error structure should then allow us to investigate the effects of signalization on travel times.

Let $tt_{d,td,i}$ be the travel time experienced by the ith probe vehicle during day d, that exited a link during time-period td. A pertinent model [the 'step-function' model] for this case is

$$\begin{aligned} tt_{d,td,i} &= \gamma + \sum_{d} \alpha_d I_{d,i} + \sum_{td} \beta_{td} I_{td,i} + \epsilon_i \\ \text{s.t.} \quad & \sum_{d} \alpha_d = 0 \\ & \sum_{td} \beta_{td} = 0 \end{aligned} \tag{5}$$

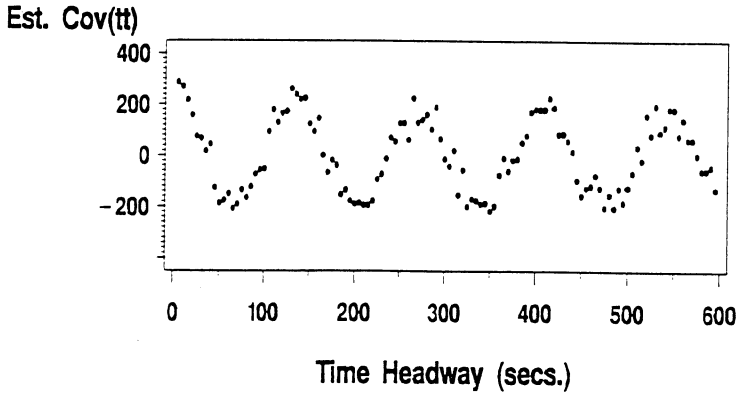

(A). Estimated Covariance against Vehicle Headways.

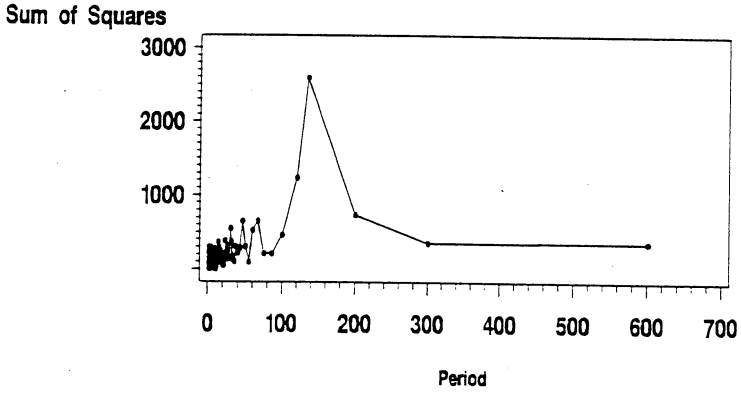

(B) Periodogram of Estimated Covariance.

Figure 2: Estimated Covariances and Signal Cycle Periodicity Apparent in Error Structure

where

$$I_{d,i} = \begin{cases} 1 & \text{if } tt \text{ was incurred on day } d \\ 0 & \text{otherwise} \end{cases}$$

and

$$I_{td,i} = \begin{cases} 1 & \text{if } t \text{ occurred during time interval } td \\ 0 & \text{otherwise} \end{cases}$$

and td is 5 minutes. The parameters α_d and β_{td} are respectively day effects and time-of-day (used as a surrogate for link volume diurnal pattern) effects experienced by the ith probe. We estimated this model by least squares [$s = 26, R^2 = .28$]. Assuming the time-of-day effect lets us subtract

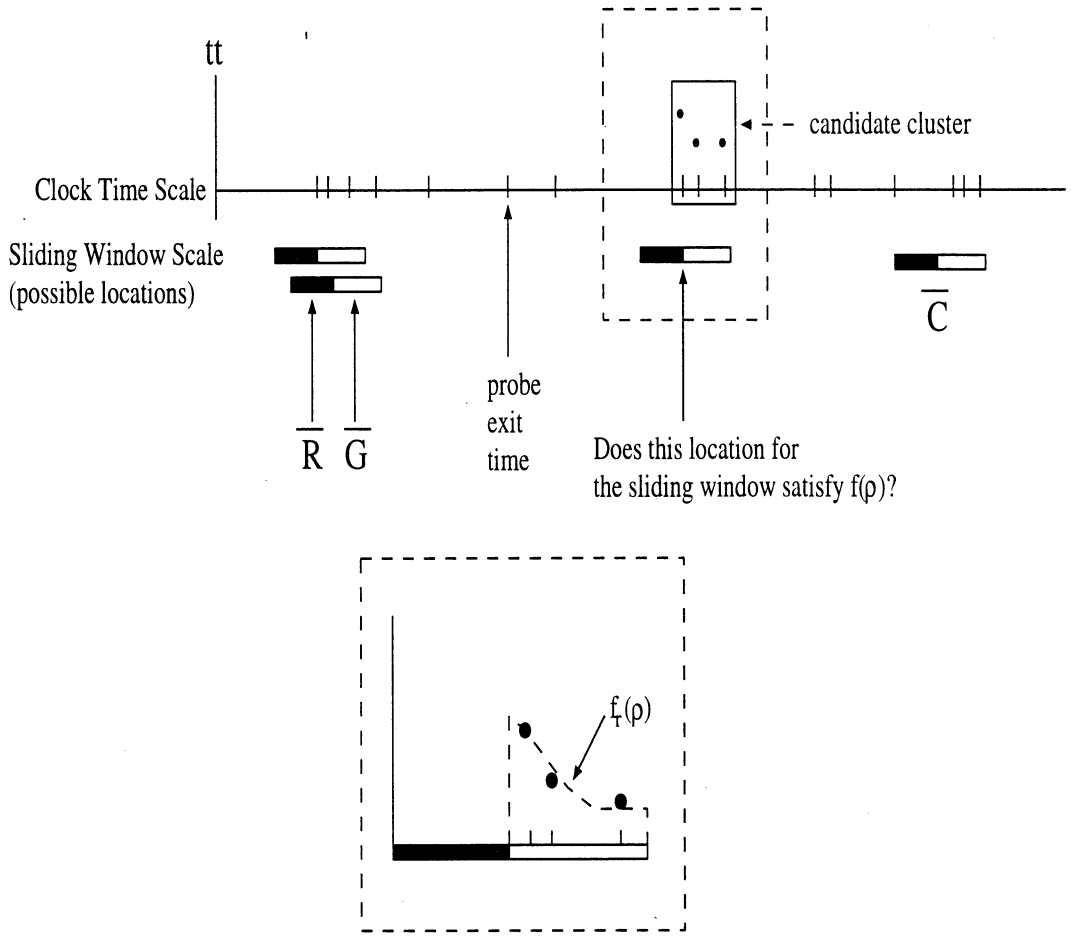

Figure 3: Basic principle of the Signal Cycle Sequence Imputation Algorithm.

out one of the major contributors to variability in travel times, that is volume, the error structure of (5) should reflect the contribution of the periodic structure imposed on estimated link travel times by signalization.

Figure 2(A) shows a plot of the time headway or the difference in exit times (on the same day d) between two probe vehicles i and j on the horizontal axis. The vertical axis gives an empirical covariance, $\widehat{\text{Cov}(tt_i, tt_j)}$, (that is, it is the product of the residuals, $e_i \times e_j$, $i \neq j$, obtained from estimating the model given in (5)). The pattern shows that two pairs of vehicles that exit at certain headways are more likely to have the same estimated covariance, than those pairs that exit at other headways. Clearly, there is a cyclical pattern left in the estimated covariance, that cannot be accounted for by subtracting out the day and time-of-day effect only from the travel time observations. This cyclical pattern is imposed by signalization.

One of the purposes of using the estimated covariance was to transform the original unequally-spaced probe data into an equally-spaced design. A periodogram of the estimated covariance (presented in Figure 2(B)) lets us see that the largest periodogram ordinate is estimated at 135 seconds. This is, in fact, very close to the actual average signal cycle length ($\bar{C} = 134.78$), which we were able to corroborate with the information on signals obtained from the video data. We have used this estimate to obtain the simulated function $f_r(\rho)$ in Section 3.2 and also as one of

the inputs in the signal cycle imputation algorithm.

3.2 IMPUTING SEQUENCE OF SIGNAL CYCLES

In this section, we describe the algorithm that is used to impute the sequence of signals (the clock times of the onset of signal cycles, which starts with the red phase, r, and the onset of green phase, g). The algorithm yields an aperiodic sequence of cycle start times (that is, cycle lengths deviate from $\bar{C}$, thus simulating the aperiodicity imposed by the demand-actuated nature of the Closed Loop Signal Control system). However, the green split is always a constant fraction of the imputed cycle length.

Figure 3 presents the underlying idea of the signal cycle sequence imputation algorithm. We use probe vehicle exit times on a continuous clock time scale and a sliding window scale, the width of which is $\bar{C} = \bar{R} + \bar{G}$, or the average signal cycle length and the height of which is $f_r(\rho)$. The sliding window scale is moved along the clock time scale to *candidate clusters* of *consecutive* probe exit times. Probe exit times form a candidate cluster if it is feasible for all points within the cluster to exit within the length $\bar{G}$. Thus, the largest distance between the outermost points in a candidate cluster cannot be greater than the available green time, in this case, $\bar{G}$.

We then analyze the tt value of the first (in time) probe report within each cluster in terms of $f_r(\rho)$. Based on some rules, we assign this tt value into one of three *bins*. Bins are defined by the estimated knot points ($\hat{\mu}_1$ and $\hat{\mu}_2$) in $f_r(\rho)$ and they identify feasible values of tt. If tt falls into one of the three bins defined by $f_r(\rho)$, then a value, $\hat{\rho}$, within the bin is selected for that travel time observation and the clock time at which the cycle starts then is simply the difference between the exit time of that probe report and $\hat{\rho}$. This value of $\hat{\rho}$ is called *hook*. Once we know the start of the signal cycle for that candidate cluster, we start building the sequence of signal cycles backward and forward in time, with exactly periodic cycle lengths. Simultaneously, we keep track of the $\hat{\rho}$ values corresponding to each and every probe report. If $\hat{\rho} \leq \bar{R}$ or the average length of the red phase for any probe observation, then we *reset* the sequence of cycles, such that $\hat{\rho}$ lies between the start of the green phase and the end of the cyle. Hence, the method yields a sequence of signal cycles that is aperiodic, the aperiodicity being introduced by the feasibility of $\hat{\rho}$ values.

There are 3 feasibility conditions for this problem:
(1) $\hat{\rho}_i \geq \bar{R}$
(2) $\hat{\rho}_i \leq \bar{C}$
(3) $tt_j \leq tt_i \quad \forall \quad \hat{\rho}_j > \hat{\rho}_i, \quad i, j \in [g_i, c_i]$.

Constraints (1) and (2) ensure that within each cycle, exits can occur in the green phase only. Constraint (3) ensures that exits that occur earlier in the cycle have travel time values that are greater than or equal to travel times that occur later in the cycle. Constraint (3) implies that tt is a decreasing function of ρ within each green phase, with a lower bound imposed by the free flow link travel time.

We now define the algorithm in detail.

As before, let $\{tt_{1,d}, tt_{2,d} \ldots, tt_{N,d}\}'$ be a vector of probe travel times on day d and let $\{t_{1,d}, t_{2,d} \ldots, t_{N,d}\}'$

be the vector corresponding probe exit times indexed on a continuous clock.

The steps in signal imputation algorithm are as follows:

1. Preliminaries:

   (a) Estimate $\bar{C}$ or the average signal cycle length via the procedure outlined on Section 3.1.

   (b) Obtain knot points $\hat{\mu_1}$ and $\hat{\mu_2}$ that give the estimated relativized exit time at which a transition from stopped delay to queueing delay and then to free flow conditions. Identify bins $\{b_1, b_2, b_3\}$ given by $b_1 = \{\bar{R}, \hat{\mu_1} - 1\}$, $b_2 = \{\hat{\mu_1}, \hat{\mu_2} - 1\}$ and $b_3 = \{\hat{\mu_2}, \bar{C}\}$.

   In Section 2, we estimated these knot points based on real signal data. Presumably for most applications, actual signal data will not be available. Therefore, for the purposes of the application of this algorithm, we have estimated the knots based on data obtained by simulation of link travel times. The details of the simulation program is desribed in Thakuriah and Sen (1996). For this particular application, the inputs to the simulation are average cycle length, green splits, arrivals per cycle and service time per cycle. The average arrival volume to cycle capacity (v/c) ratio simulated (for 10 simulated 'days') was 0.58. The outputs are travel times of individual vehicles and ρ values. We estimated $f_r(\rho)$ using the simulated data by the functional form as in equation (1), by nonlinear least squares, that yielded $\hat{\mu_1} = 81$ seconds and $\hat{\mu_2} = 108$ seconds. Note that these values are lower than those estimated using the actual probe travel time and signal data (given in Table 1), but that is to be expected because in the simulation, we only considered cases of undersaturated cycles with uniform or red phase vehicular delay.

2. The Algorithm (we drop d from the subscript with the understanding that the procedure uses data for one day at a time):

   (a) Calculate the time difference among each two probe reports, that is between $\{t_n, t_{n-1}\}$, $\{t_n, t_{n-2}\}$ $\ldots$ $\{t_n, t_{n-i}\}$, $i = 1, \ldots, n$. Call these values $\zeta_{n,n-1}$, $\zeta_{n,n-2}$, $\ldots$, $\zeta_{n,n-i}$.

   (b) If $0 \leq \zeta_{n,n-1} \leq \ldots \zeta_{n,n-i} \leq \bar{G}$, then the vector of travel time reports $\{tt_{n-i}, \ldots, tt_n\}'$, is a candidate cluster, $\omega_{n-i} \in \Omega$. A candidate cluster, as defined earlier, is a set of probe reports (*that are consecutive in time*) that lie within a time interval which is less than or equal to the average length of the green phase and is indexed by the first observation (in time) in the cluster. A candidate cluster must consist of at least two consecutive probe reports. Naturally, there may be several candidate clusters in one day. Also, the same probe report may be in several different candidate clusters.

   (c) For each candidate cluster, $\omega_{n-i} \in \Omega$, do the following

   I. Fit hook for t_{n-i} or the exit time of first observation (in time) in a cluster. Fitting a hook refers to assigning a ρ value to the observation. The hook is fitted based on tt_{n-i}, the estimated function $f_r(\rho)$, and the bin into which tt_{n-i} value as explained below.

   The estimated function $f_r(\rho)$ allows the assignment of a bin value corresponding to tt_{n-i}. We choose the placement of the hook in the selected bin via Monte Carlo. We assume that ρ_{n-i} is uniformly distributed in the selected bin and sample ρ_{n-i} from

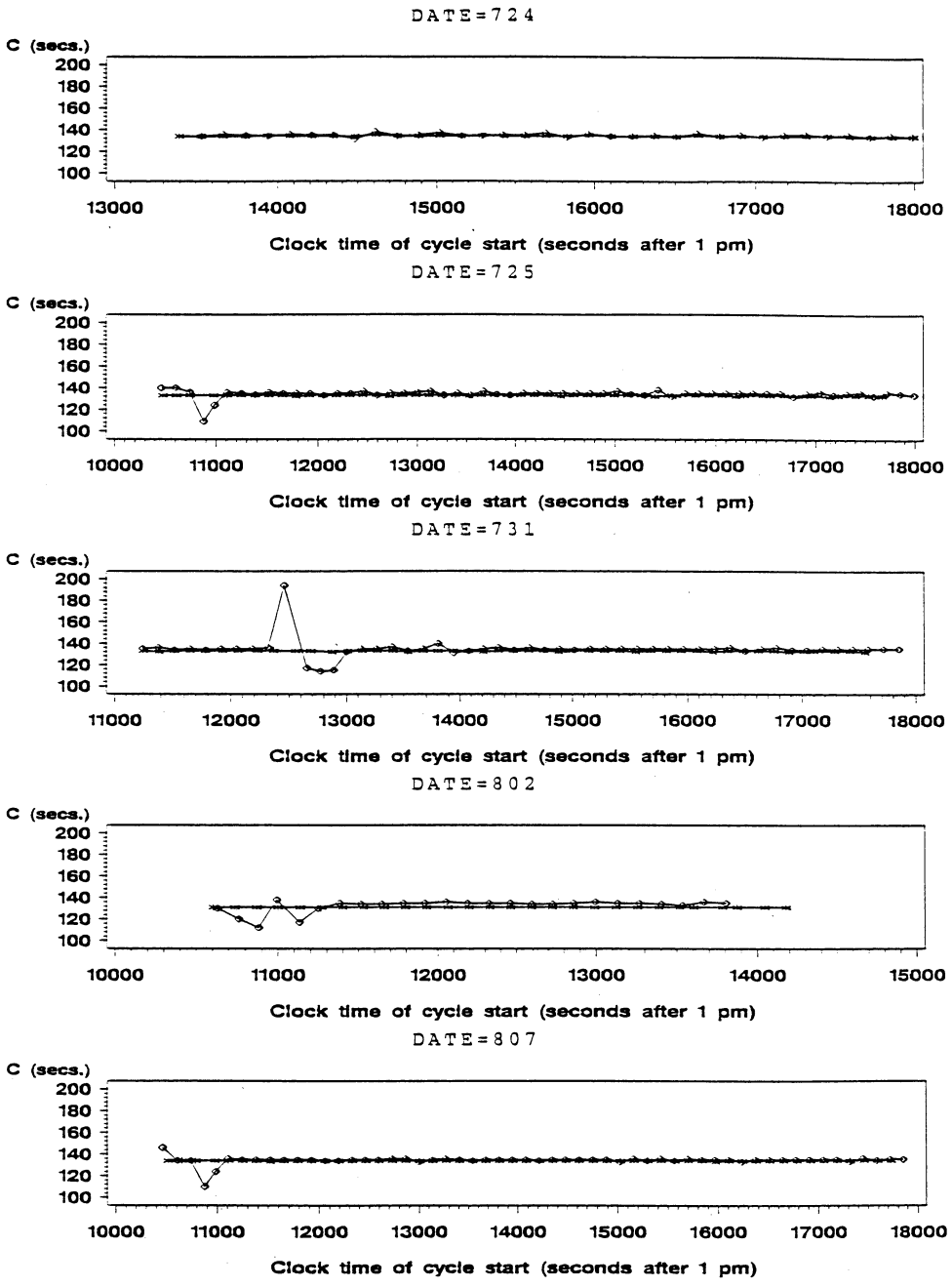

◇: Start time of actual signal cycles (onset of actual red phases).

∗: Start time of imputed signal cycles (onset of imputed red phases).

Figure 4: Imputed and Actual Cycle Sequence for 5 days.

this distribution. The reason for using Monte Carlo as opposed to a straightforward inverse transformation of $tt_{n-i} \rightarrow f_r(\rho) \rightarrow \rho_{n-i}$ is that the flat part of the estimated $f_r(\rho)$ is totally uninformative about ρ in the bin $\{\mu_2, \bar{C}\}$.

Once ρ_{n-i} is selected, the start time of the cycle is simply $r_{n-i} = t_{n-i} - \rho_{n-i}$.

II. Build cycles with exact periodicity, $\bar{C}$, backward and forward in time from t_{n-i}.

III. Calculate $\rho_{n'} = t_{n'} - r_{n'}$ $\forall$ $n' \neq n - i$, where $r_{n'}$ is the start of the imputed cycle to which n' belongs. If $\rho_{n'} < \bar{R}$ for any $t_{n'}$, the cycle, $r_{n'}$, to which the observation belongs is offset such that $\rho_{n'} \geq \bar{R}$. The offsetting introduced depends on whether $t_{n'} > t_{n-i}$, the point at which we start building the cycles, or $t_{n'} < t_{n-i}$.

If $t_{n'}$ is earlier in time than t_{n-i} then the offset is obtained by examining $tt_{n'}$ and pushing the start of the cycle, $r_{n'}$, backward in time such that the criteria $\rho_{n'} \geq \bar{R}$ is satisfied. If $t_{n'}$ is later in time than t_{n-i}, then $tt_{n'}$ indicates by how much the length of the last cycle should be extended in order to include $t_{n'}$ in that cycle.

(d) Continue building the ladder till all observations on day d are inside imputed cycles.

(e) After the sequence of cycles, $\{C(\omega_{n-i})\}$, is built for candidate cluster ω_{n-i}, we have a vector of imputed values $\{\hat{\rho_1}, \ldots, \hat{\rho_N}\}$, corresponding to ω_{n-i}. We then estimate the relationship $tt_i = f(\hat{\rho_i}) + \epsilon_i$ and computed the Mean Square Error, $s^2 = \sum_{i=1}^{N}(tt_i - \hat{tt}_i)/(N-2)$.

3. Build cycle sequences for all identified candidate clusters in the same way on day d and compute s^2 for all clusters.

4. The selected cycle sequence is the one generated by cluster ω for which s^2 is the minimum over all $\omega \in \Omega$.

4 APPLICATIONS

We now present some applications of the signal cycle imputation algorithm for the purpose cycle sequence tracking (in Section 4.1), for travel time estimation (in Section 4.2) and 'real-time' prediction (Section 4.3) of travel time. In each case, the real data are presented along with the estimated for comparative purposes.

4.1 TRACKING THE CYCLE SEQUENCE

Figure 4 shows the imputed sequence of signal cycles based on the method in Section 3.2 for five days for which we have actual signal data. Each plot is for one day, labeled 724 for July 24 and so on. The figure shows the actual and imputed start times of red phases on a continuous clock on the horizontal axis and the cycle length of the actual and imputed cycles on the vertical axis. The imputed cycles are from the best fit cycle sequence according to the criteria developed in

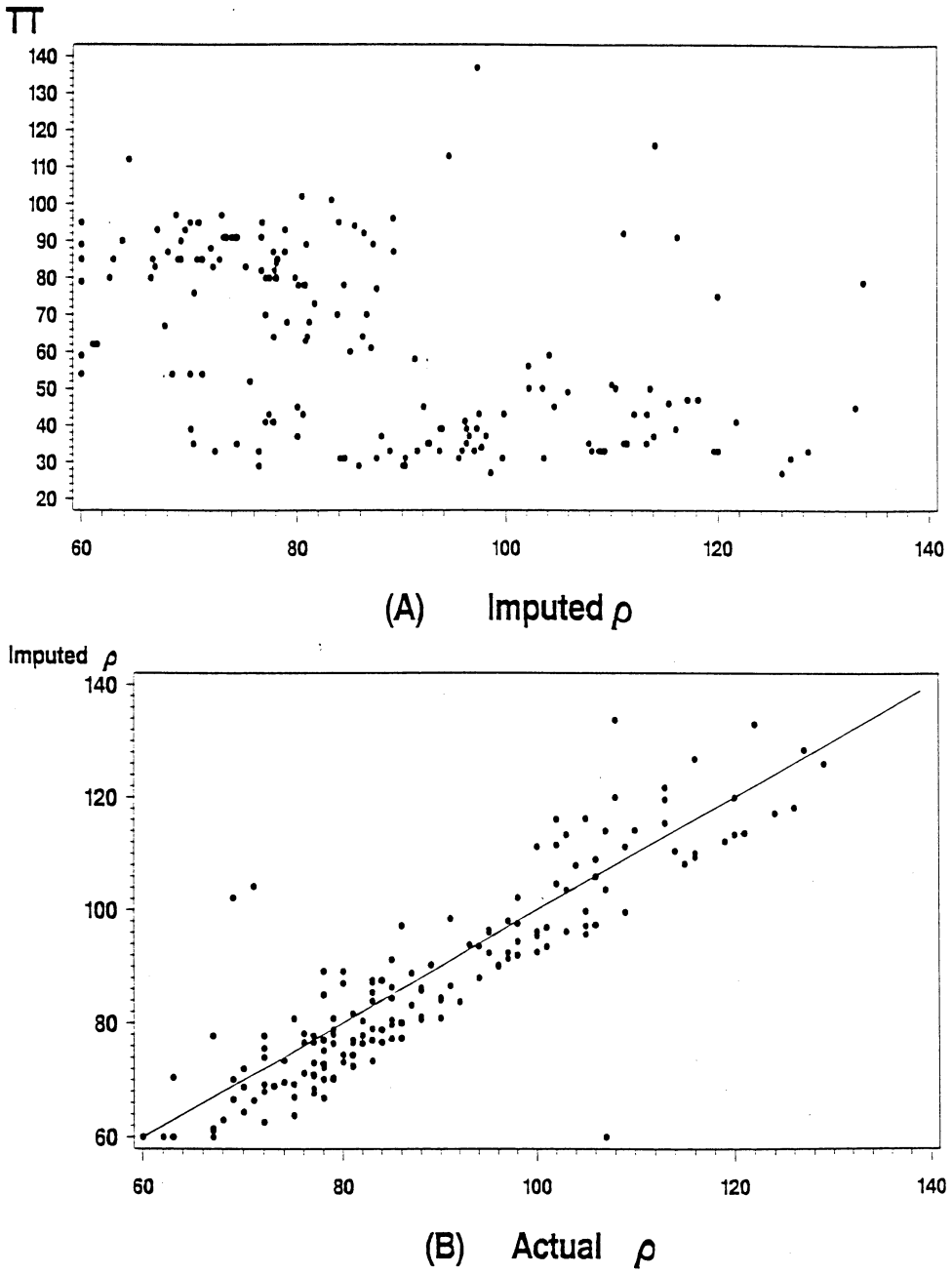

(A). Travel Time and Imputed ρ.

(B). Actual ρ and Imputed ρ.

Figure 5: Estimation of Relativized Exit Time ρ.

Estimates:	$\hat{\alpha}$=77.81	$\hat{\beta}_1 = -0.69$	$\hat{\beta}_2 = 0.69$
Knot:	$\hat{\Gamma} = 62$ secs.		
Slopes:	Part 1: -0.69	Part 2: 0	
Fit:	s=9.90	R^2=.84	

Table 2: Estimates from model of travel time as a function of imputed relativized entry time γ.

Section 3.2, Item 4. Note that the scale of the two axis are very different. The important fact to note is that the cycle start times should lie along a vertical line drawn from the horizontal axis.

The fit is clearly better on some days than on others. On July 24, the imputed cycle sequence follows the actual almost exactly. On July 25, the imputed signal cycle sequence is always ahead of the actual sequence by one or two seconds. This was also the day on which the minimum number of resets were done. If no resets are done, then the actual and the imputed cycles will always be off by a constant amount, if the actual cycles are exactly periodic (the imputed cycles are always exactly periodic if no resetting is done). But for most days, the actual and the imputed cycle start times lie fairly close to vertical lines drawn from the horizontal axis.

4.2 TRAVEL TIME ESTIMATION

Figure 5(A) shows travel times plotted against the estimated ρ_i, based on the signal cycle sequence reconstruction (the results of which are presented in Section 4.1). Figure 5(B) shows a comparison of the imputed ρ_i's against the actual ρ_i's.

The pattern presented in Figure 5(A) is very similar to that obtained on the basis of real signal data, shown in Figure 1. However, the entire imputed pattern in Figure 5(A) is shifted a little more to the left (toward the start of the green phase) than the actual pattern. Also we see from Figure 5(A), that the imputed ρ_i's underestimates the actual ρ_i's slightly. This deviation of the imputed ρ_i's from the actual indicates that the estimated function $f_r(\rho)$ that we used for allocating the tt_i's to ρ_i's, underestimates the function that would have been pertinent for the level of volume in some cycles. As we had discussed in Section 3.2, the estimated function $f_r(\rho)$ is relevant for the undersaturated cases with uniform (red phase) delay only, under the condition that vehicles arrive uniformly within the red and green phases. This result points to the importance of the knowledge of volume levels in the signal imputation problam.

Once we have the imputed signal data, we are in a position to estimate travel times on the effects of signalization, without having direct measurements on signal control events. We do so by means of the following model:

Let tt_i be the travel time of vehicle i entering the link at time $ent_i = t_i - tt_i$ on day d, time-of-day td and average signal cycle period $\bar{C}$. Our purpose is to estimate $tt_i = g(\gamma_i) + \epsilon_i$ where $\gamma_i = ent_i \text{modulo}(r_i^e)$ where r_i^e is the estimated start of the cycle (obtained by applying the signal cycle imputation problem) in which the $i$the probe exited. The exact model (the imputed signal cycle model) estimated (by non-linear least squares) is:

$$tt_i = \alpha + \beta_1 \gamma_i + \beta_2 (\gamma_i - \Gamma)\delta + \epsilon_i \tag{6}$$

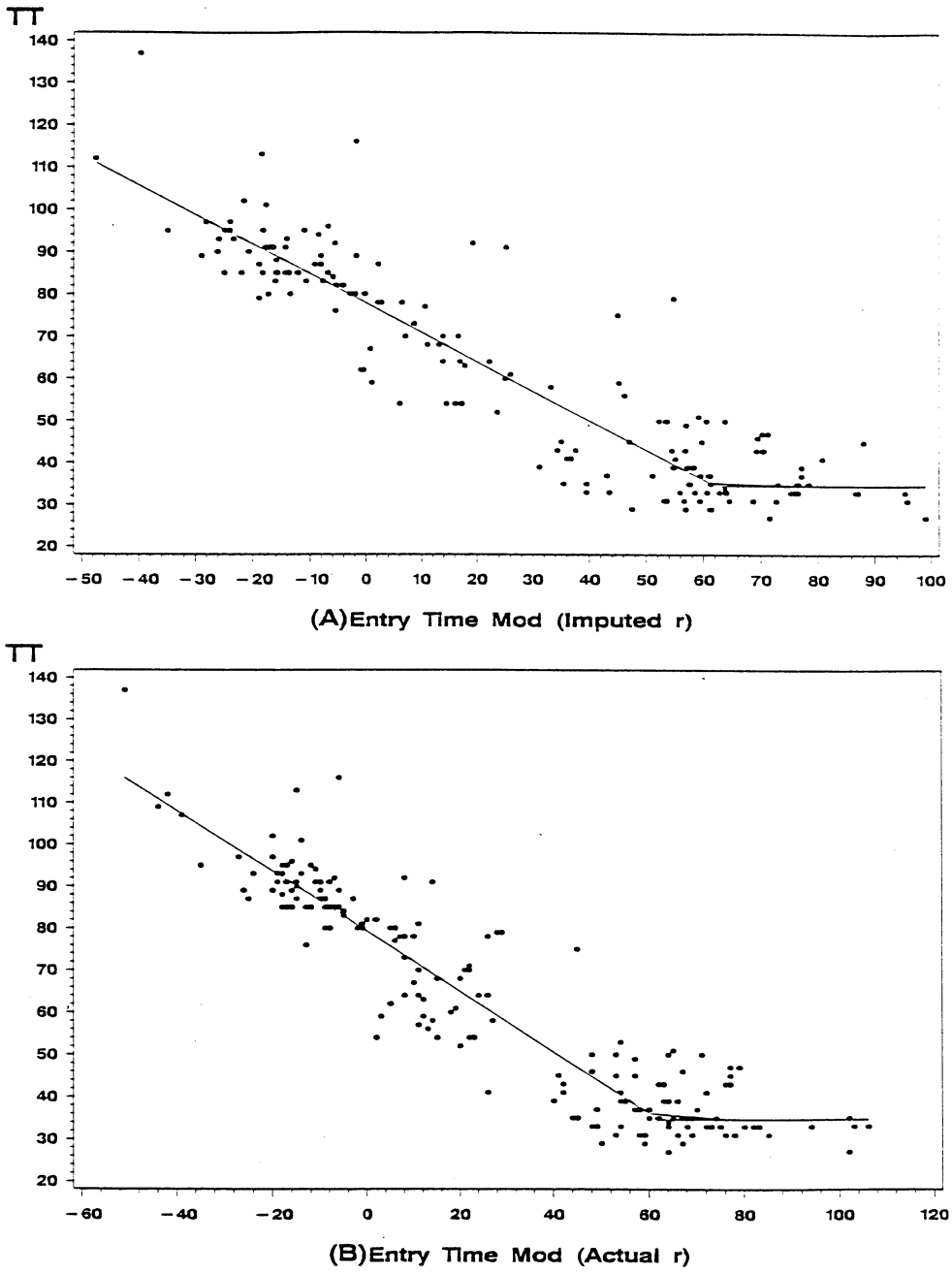

(A). Travel Time and Imputed γ.

(B). Travel Time and Actual γ.

Figure 6: Estimation of Travel Time as a Function of Relativized Entry Time γ.

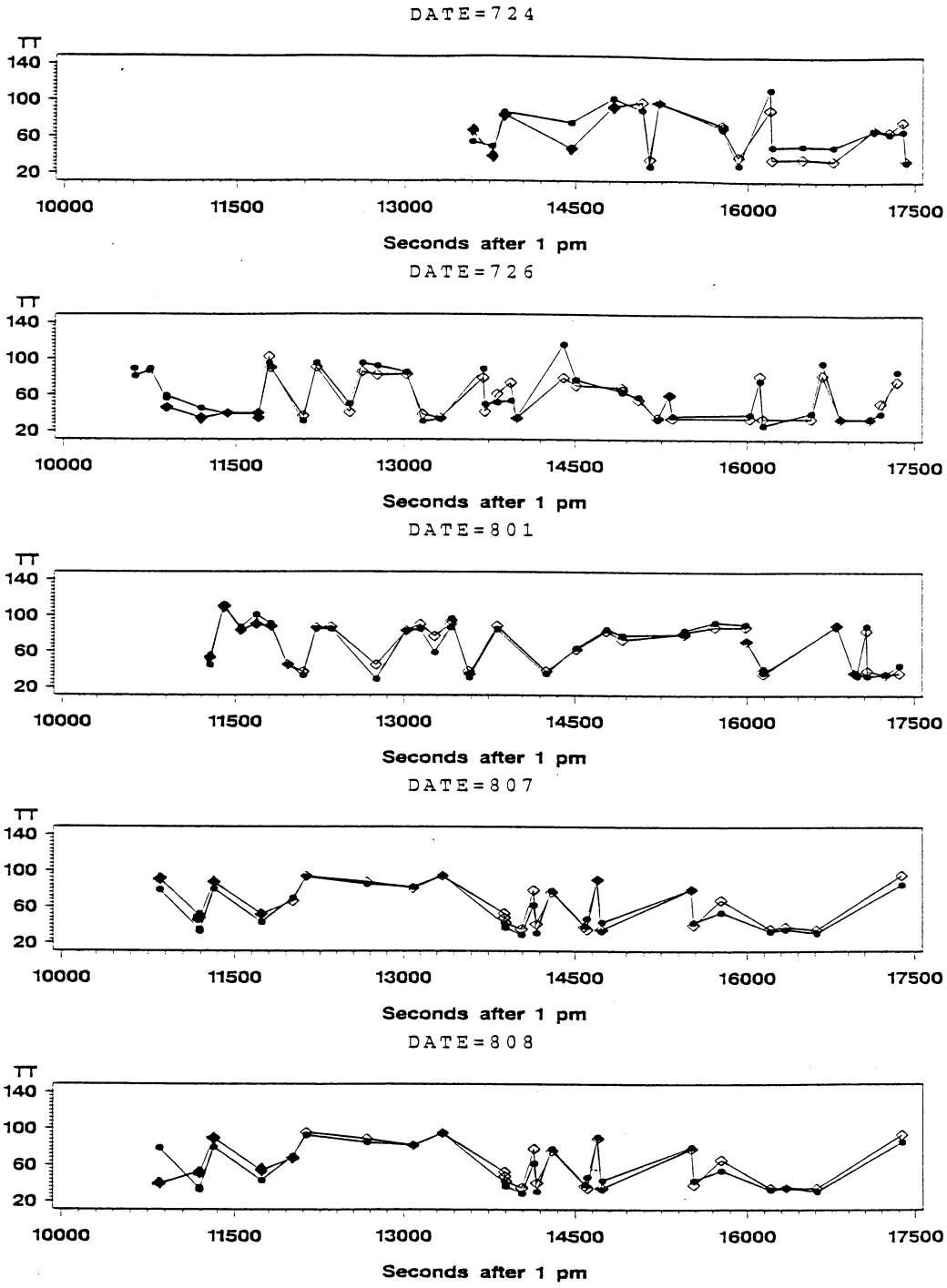

•: Actual *tt*.

◇: Predicted *tt*.

◆: 'Predicted' *tt* from backward cycle sequence building.

Figure 7: Dynamic Link Travel Time Prediction.

•: Actual *tt*.

◇: Predicted *tt*.

◇: 'Predicted' *tt* from backward cycle sequence building.

Figure 7: Dynamic Link Travel Time Prediction.

$$\text{s.t.} \quad \beta_1 + \beta_2 = \frac{\text{link length}}{\text{speed limit}}$$

where

$$\delta = \begin{cases} 1 & \text{if} \quad \gamma_i > \Gamma \\ 0 & \text{otherwise} \end{cases}$$

and where the knot point Γ was a parameter in the model. Table 2 presents the estimates of the model and Figure 6(A) presents the fit. For comparative purposes, tt as a function of the actual γ_i's is shown in Figure 6(B).

We see that using the imputed signal information to estimate travel times offers a marked improvement (in terms of the Root Mean Square Error) over the 'step-function' travel time estimation model given in equation (5) ($s = 9.90$ for the imputed cycle travel time model and $s = 26$ for the step function model).

Signal cycle imputation can further help to improve the estimates from the step-function model. As mentioned in the introduction, if a term reflecting the effect of signalization is left out from a model of travel time, the estimates of travel time may be biased. Because the step-function model averages over travel times in fixed time intervals (in the case of the model in equation (5, $td = 5$ minutes) one interval may contain a longer part of green phases than the next 5-minutes. The result of this aggregation may be that one interval has a lower estimate of expected travel time simply because of arbitrary temporal aggregation and not because of true covariate effects. This implies that the estimates of that model may be biased (Sen *et al.* 1996). If we wanted estimates of expected link travel times as step-functions of clock time, then the interval should be over an integer multiple of the cycle length, thereby avoiding bias in the estimates of travel time.

4.3 TRAVEL TIME PREDICTION

The dynamic link travel time prediction problem is: given a vector of travel time data, $\{tt_1, tt_2, \ldots, tt_n\}$, upto time t, predict travel time $tt(\widehat{t+\delta})$ at a future time $t + \delta$. The time $t + \delta$ is the estimated entry time of a vehicle into the link.

In this section, we present the results from the real-time forecasting of travel time. Our predictions are conditional on day-type, time-of-day, average cycle periodicity and imputed sequence of signal cycle. The predicted travel times were obtained as follows:

1. Use data for 3 days to impute signal cycle sequence.
2. Use travel time and imputed data for the same three days to estimate the model in equation (6).
3. Obtain dynamic forecasts for data from five other days. The results are shown in Figure 7. The steps are:
   (a) build signal cycle sequence on day d based on data upto time t; for each day, these were based on four or five points that are shown in black diamonds in Figure 7
   (b) extend signal cycle with exact periodicity upto the entry time $(t+\delta)$ of the next probe, j

$e_i = tt_i - \hat{tt}$ (seconds)	Frequency
-20 to -11	18
-10 to -1	50
0	11
1 to 10	50
11 to 20	10
21 to 30	3
31 to 40	4

Table 3: Distribution of errors from dynamic link travel time predictions.

(c) obtain $\gamma_j = (t + \delta)\text{modulo}(r_j^e)$

(d) once γ_j is known, the prediction $\hat{tt}_j$ is then obtained from the previously estimated relationship at Step 2 by inverse transformation.

4. Once probe j exits the link, its actual tt and exit time t is used to reset the signal cycle sequence as necessary as discussed earlier.

The first few travel time observations on each day (shown in black diamonds) are used to build the signal cycle sequence each day backward in time (as discussed in Section 3.2, Item 2 II). Once the hook is fitted based on one of these observations, we start to build the cycle sequence forward in time. From that point onwards, we use only the entry times of probe vehicles as data input in the prediction procedure. For each probe entry time (in terms of clock time), we make a prediction. The output of the prediction procedure, for each probe observation considered, is a predicted value and a reset of the signal cycle sequence when necessary. The figures show that the number of observations on each day is very small. The procedure, therefore, is capable of making predictions based on extremely sparse data, for intermittent time horizons into the future and is not constrained into making predictions in fixed time-steps. It requires a number of covariate information, but it also demonstrates that on signalized arterials, perhaps the major covariate for predictive purposes is signal information.

Figure 7 shows that the procedure does well in predicting the travel times of probe vehicles on a link, given its entry time into the link. Table 3 gives the distribution of $e_i = tt_i - \hat{tt}_i$. There are 18 observations for which $e_i = 0$. About 76% of the travel time observations were predicted to within ± 10 seconds and about 95% were predicted to within ± 20 seconds. The points with the largest errors were from cycles with average $v/c \geq 0.85$.

5 CONCLUSIONS

The effect of signals and volumes are fundamental covariates of link travel time. However, data on the periodic sequence of signal cycles are not likely to be available in most ATIS and ATMS. In this paper, we used measurements of link travel time and link exit times to impute the aperiodic sequence of signal cycles. We then used this imputed sequence as input into the estimation of travel time and for the dynamic prediction of link travel times. We did so by assuming that the relationship between travel time and exit time relativized to within the signal cycle (ρ) that

holds for undersaturated cycles with uniform (within-phase) arrivals holds for all cycle saturation conditions considered. The results indicate that this approximation is quite reasonable. In terms of the Root Mean Square Error, imputing signal cycles and using this information as a conditioning variable in estimating travel times is a marked improvement over a step-function type estimation of travel time, where travel time is considered to be a function of volume (in terms of a time-of-day diurnal pattern) alone. Moreover, the imputed sequence of signal control allows extremely reasonable 'real-time' predictions of link travel times.

6 REFERENCES

1. Boyce, D. E., A. M. Kirson and J. L. Schofer (1994). ADVANCE — The Illinois Navigation and Route Guidance Demonstration Program. In *Advanced Technology for Road Transport*, Ian Catling (ed.), Artech House, Boston.

2. Daley, D. J. (1996). Some Statistical Properties of Link Travel Times. *Technical Report No. 44*, National Instirute of Statistical Sciences, May.

3. Liu, N. and A. Sen (1994). Dynamic Travel Time prediction in ADVANCE: Modified Release 1.5 TTP Algorithm Report and Detail Design Document (#8600). *ADVANCE Working Paper Series*, No. 48, Urban Transportation Center, University of Illinois, Chicago.

4. Rouphail, N. M. and N. Dutt (1995). Estimating Travel Time Distributions for Signalized Arterials: Model Development and Potential Applications. Submitted for publication in *Proceedings of the 4th Annual Meeting*, IVHS America, Washington, D.C., March 15-17, 1995.

5. Sen, A. and P. Thakuriah (1995). Estimation of Static Travel Times in a Dynamic Route Guidance System. In Network, Control, Communication and Computing Technologies for Intelligent Transportation Systems, a special issue of *Mathematical and Computer Modelling*, Vol. 22, Number 4–7, August–December.

6. Sen, A., P. Thakuriah, A. Karr and X. Zhu (1996). Frequency of Probe Reports and Variance of Link Travel Time Estimates. Accepted for publication in *ASCE: The Journal of Transportation Engineering.*

7. Thakuriah, P., A. Sen and A. Karr (1996a). Analysis of Probe-Based Information on Signalized Arterials. Submitted for consideration for publication in Behavioral and Network Impacts of Driver Information Systems. John Wiley and Sons.

8. Thakuriah, P. and A. Sen (1996b). An Investigation into the Quality of Information given by An Advanced Traveler Information System. To be published in *Transportation Research C.*